ISSN 1070-3284, Russian Journal of Coordination Chemistry, 2014, Vol. 40, No. 10, pp. 704–710. © Pleiades Publishing, Ltd., 2014.

Crystal Structures and Luminescence of a Series of Cadmium(II) Complexes Based on Isophorone Derivative Containing Imidazolyl[1]

W. G. Xi[a], M. D. Yang[a], L. P. Wang[b], H. J. Li[a], J. H. Yu[a], H. P. Zhou[a, *], and Z. C. Wu[a]

[a] *College of Chemistry and Chemical Engineering, Key Laboratory of Functional Inorganic Materials Chemistry of Anhui Province, Anhui University, Hefei, 230601 P.R. China*

[b] *School of Materials and Chemical Engineering, Anhui Jianzhu University, Hefei, 230601 P.R. China*

**e-mail: zhpzhp@263.net*

Received March 22, 2014

Abstract—Three new complexes, $[CdL_2(CH_3COO)_2(H_2O)_2]$ (**I**), CdL_2Br_2 (**II**), CdL_2I_2 (**III**), have been successfully synthesized by self-assembly of corresponding metal salts with (*E*)-2-(3-(4-(1*H*-imidazole-1-yl)styryl)-5,5-dimethylcyclohex-2-enylidene)malononitrile (L). The structures of the complexes were determined by single crystal X-ray diffraction analysis (CIF file CCDC nos. 957831 (**I**), 957792 (**II**), 957832 (**III**)). In complex **I**, central metal is six-coordinated and the crystal packing shows a 3D supramolecular framework. Complexes **II** and **III** display the similar 2D supramolecular structures in which the central metals are four-coordination. The luminescent properties were investigated.

DOI: 10.1134/S107032841410011X

INTRODUCTION

Over the past decade, the design and synthesis of supramolecular complexes have attracted great interest due to their intriguing structural architectures and potential applications in catalysis, gas storage, chemical separation, photoluminescence, and so on [1–6]. Up to now, a number of supramolecular complexes with specific topologies and excellent properties have been synthesized by assembly of metal salts and organic ligands [7, 8]. The structural types of the resulting supramolecular complexes are affected by factors such as organic linkers, pH value, solvent, temperature, and so on [9–14]. Among them, the metal ions and anions are based-control factors. It is well known that different metal ions possess different properties and coordination modes, which play key roles in the formation of both molecular structures and packing structures of complexes [15, 16]. Plenty of studies have shown that Cd^{2+} ion may adopt different coordination modes, such as four-, five- or six-coordination modes according to the specific structures of the different ligands [17, 18]. The introduction of different small anions can also have a significant effect on the structural construction of complexes and their properties [18, 19]. It is important for synthesizing target materials to understand the role of the above factors in self-assembly process.

Without a doubt, the organic ligands can control the properties and topology of coordination complexes. The multidentate π-conjugated ligands have been most extensively used due to their good optical properties and coordinating with metal centres in various modes. We designed and synthesized the ligand (*E*)-2-(3-(4-(1*H*-imidazole-1-yl)styryl)-5,5-dimethylcyclohex-2-enylidene)malononitrile (L) which contain a π-conjugated system and imidazolyl as well as dicyanoisophorone groups. Schematic drawing of the ligand is shown below:

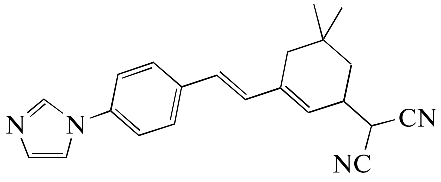

(L)

In order to evaluate the role of anions in the self-assembly process and the optical properties, we prepared three new complexes $[CdL_2(CH_3COO)_2(H_2O)_2]$ (**I**), CdL_2Br_2 (**II**), CdL_2I_2 (**III**). The crystal structures and solid state luminescent properties were investigated in detail.

EXPERIMENTAL

General methods. All the reagents and solvents were commercially available and used without further purification. IR spectra were recorded from KBr discs in the 4000–40 cm^{-1} range on a Nicolet Nexus 870 spectrophotometer. Elemental analyses were carried out on Vario EL analyzer. The solid state luminescence spectra were measured on the Hitachi F-7000 fluorescence spectrophotometer. In the measurements of emission and excitation spectra, the pass width is 5 nm

---

[1] The article is published in the original.

for complexes **I**, **II**, and **III**. For time-resolved fluorescence measurements, the fluorescence signals were collimated and focused onto the entrance slit of a monochromator with the output plane equipped with a photomultiplier tube (HORIB FluoroMax-4P). The decays were analyzed by least-squares. The quality of the exponential fits was evaluated by the goodness of fit (χ^2).

Synthesis of L was carried out as described in [20].

Synthesis of complex I. A methanol solution (10 mL) of $Cd(CH_3COO)_2$ (0.051 g, 0.22 mmol) was carefully layered onto a solution of L (0.15 g, 0.44 mmol) in chloroform (10 mL). Yellow, block crystals were obtained by diffusing the methanol solution into chloroform solution for a week at room temperature. The yield was 0.14 g (69%).

For $C_{48}H_{50}N_8O_6Cd$

anal. calcd., %:	C, 60.85;	H, 5.32;	N, 11.83.
Found, %:	C, 60.47;	H, 5.28;	N, 11.59.

IR bands (ν, cm^{-1}): 3339 s, 3125 s, 2950 s, 2221 v.s, 1569 v.s, 1522 v.s, 1392 s, 1337 s, 1307 s, 1271 s, 1186 s, 1159 s, 1124 s, 1064 s, 982 s, 962 s, 853 s, 819 s, 738 m, 653 m, 550 m, 496 m.

Synthesis of complex II was carried out by the same procedure used for preparing **I** except that $CdBr_2$ (0.06 g, 0.22 mmol), instead of $Cd(CH_3COO)_2$ (0.051 g, 0.22 mmol), was used as the starting material. Saffron yellow, block crystals were obtained. The yield was 0.15 g (71%).

For $C_{44}H_{40}N_8Br_2Cd$

anal. calcd., %:	C, 55.45;	H, 4.23;	N, 11.76.
Found, %:	C, 55.36;	H, 4.20;	N, 11.51.

IR bands (ν, cm^{-1}): 3426 s, 3131 s, 2928 m, 2220 s, 1796 m, 1568 v.s, 1523 v.s, 1501 s, 1399 s, 1367 s, 1331 s, 1308 s, 1269 s, 1190 s, 1129 s, 1066 s, 975 s, 962 s, 876 m, 853 m, 817 m, 741 m, 642 m, 549 m.

Synthesis of complex III was fabricated by the same procedure used for the preparation of **I** except that $Cd(CH_3COO)_2$ was replaced with CdI_2 (0.08 g, 0.22 mmol). Yellow, block crystals were obtained. The yield was 0.15 g (65%).

For $C_{44}H_{40}N_8I_2Cd$

anal. calcd., %:	C, 50.47;	H, 3.85;	N, 10.70.
Found, %:	C, 50.57;	H, 3.93;	N, 10.61.

IR bands (ν, cm^{-1}): 3406 s, 3129 s, 2953 s, 2926 m, 2220 v.s, 1566 v.s, 1523 v.s, 1501 s, 1398 s, 1367 s, 1332 s, 1308 s, 1268 s, 1190 s, 1161 s, 1128 s, 1065 s, 975 s, 962 s, 939 s, 877 s, 852 s, 817 s, 736 m, 642 m, 549 m.

X-ray crystallography. The X-ray diffraction measurements were performed on Bruker SMART CCD area detector using graphite monochromated MoK_α radiation ($\lambda = 0.71069$ Å) at 298(2) K. Intensity data were collected in the variable ω-scan mode. The structures were solved by direct methods and difference Fourier syntheses. The non-hydrogen atoms were refined anisotropically and hydrogen atoms were introduced geometrically. Calculations were performed with SHELXTL program package [21]. Details of the crystal parameters, data collections and refinements are listed in Table 1, and selected bond distances and angles are given in Table 2.

Crystallographic data for the structures reported in this paper have been deposited with the Cambridge Crystallographic Data Centre as supplementary publication (no. 957831 (**I**), 957792 (**II**), 957832 (**III**): deposit@ccdc.cam.ac.uk or http://www.ccdc.cam.ac.uk/data_request/cif).

RESULTS AND DISCUSSION

In complex **I**, Cd^{2+} ion is six-coordinated two O atoms of acetate anions, two N atoms of the imidazolyl groups from two ligands and two coordinated water molecules, to form a slightly distorted octahedral geometry (Fig. 1a). The bond angles around the Cd^{2+} ion are in the range of 87.56(8)°–180.00(9)°.

As shown in Fig. 1b, the neighboring molecules are linked by intermolecular O(3)$^{\#1}$–H(3*B*)$^{\#1}$···O(2), C(22)–H(22)···O(2) hydrogen bonding interactions and C(5)–H(5*A*)···π interactions into one-dimensional chains along the *x* axis. The distances of H(3*B*)$^{\#1}$···O(2), H(22)···O(2) and H(5*A*)···centroid are 2.14, 2.48, and 2.76 Å, respectively. In addition, the intramolecular hydrogen bonding interactions occur between O(1) and H(3*A*), the distance of H(3*A*)···O(1) is 1.81 Å and the angle of O(3)–H(3*A*)···O(1) is 156°, which form a coplanar six-member ring with C(23), O(2), Cd(1), and O(3). Two nitrogen atoms of cyano in one ligand are not directly involved in coordination, but play an important role in the formation of 2D and 3D structures through C–H···N hydrogen bonding interactions. As shown in Fig. 1c, the C(5)–H(5*B*)···N(1)$^{\#1}$ interactions with 2.59 Å of H(5*B*)···N(1)$^{\#1}$ and 162° of C(5)–H(5*B*)···N(1)$^{\#1}$ based on the cyano-group link the neighboring chains to form a 2D supramolecular structure. The adjacent layers are stacked through C(12)–H(12)···N(2) and C(18)–H(18)···N(2) hydrogen bonding interactions to form a 3D structures. The distances of H(12)···N(2) and H(18)···N(2) are 2.72 and 2.66 Å, respectively.

In complex **II**, the Cd^{2+} ion is coordinated with two terminal bromine ions and two N atoms of imidazolyl groups (Fig. 2a). The bond angles around the Cd^{2+} ions are in the range of 98.79(8)°–123.26(8)°.

The neighboring molecules are linked in "face to face" mode by C(9)–H(9)···Br hydrogen bonding (the distance of H···Br is 2.97 Å and the angle of C–H···Br

Table 1. Crystallographic data and structure refinement for complexes **I–III**

Parameter	Value		
	I	**II**	**III**
Formula weight	947.36	953.06	1047.04
Crystal system	Triclinic	Monoclinic	Monoclinic
Space group	$P\bar{1}$	$P2/c$	$P2/c$
a, Å	5.553(5)	18.837(9)	18.656(5)
b, Å	11.269(5)	6.467(3)	6.473(5)
c, Å	18.858(5)	18.193(9)	18.578(5)
α, deg	83.281(5)	90	90
β, deg	85.768(5)	103.025(6)	103.729(5)
γ, deg	85.061(5)	90	90
V, Å^3	1165.2(12)	2159.2(18)	2179.4(19)
Z	1	2	2
ρ_{calcd}, g cm^{-3}	1.350	1.466	1.596
μ, mm^{-1}	0.525	2.396	1.957
θ Range, deg	1.09–25.94	1.11–25.00	1.12–25.00
F(000)	490	956	1028
Reflections collected/unique	8757/4395	14702/3808	13433/3732
R_{int}	0.0167	0.0355	0.0301
GOOF on F^2	1.151	1.122	1.046
R_1, wR_2 ($I > 2\sigma(I)$)	0.0291, 0.0872	0.0325, 0.0858	0.0358, 0.1162
R_1, wR_2 (all data)	0.0307, 0.0939	0.0479, 0.1025	0.0488, 0.1389
$\Delta\rho_{max}/\Delta\rho_{min}$, e Å^{-3}	0.515/–0.326	0.975/–0.820	1.726/–1.303

is 144.37°) and C(17)–H(17*A*)···π interaction (the distance of H···centroid is 2.70 Å and the angle of C–H···centroid is 168°) to form a 1D structure along the *y* axis (Fig. 2b). In the *yz* plane, the molecules are also interconnected by C(10)–H(10)···N(3) hydrogen bonding interactions (the distance of H···N is 2.57 Å and the angle of C–H···N is 154°) to aggregate in a 2D net (Fig. 2c).

In complex **III**, the central metal Cd^{2+} ion is four-coordinated by two terminal chlorine ions and two N atoms of pyrazolyl groups to form a slightly distorted tetrahedral geometry (Fig. 3a). The bond angles around the Cd^{2+} ions are in the range of 97.79(11)°–122.26(10)°.

The supramolecular structure of complex **III** is similar to that of complex **II** (Fig. 3). The neighboring molecules are linked by C(16)–H(16)···I hydrogen bonding interaction (H(16)···I 3.09 Å, the angle of C(16)–H(16)···I is 140°) and C(5)–H(5*A*)···π interaction (the distance of H(5*A*)···centroid is 2.69 Å, the angle of C(5)–H(5*A*)···centroid is 168°), giving rise to an extended 1D chain (Fig. 3b). The adjacent chains are stacked through C(13)–H(13)···N(2) hydrogen bonding interactions (H(13)···N(2) 2.658 Å, the angle of C(13)–H(13)···N(2) is 150°) to form 2D supramolecular structure (Fig. 3c).

From the crystal structure of Cd(II) complexes containing imidazolyl ligands have been reported, we can find that the central cadmium ion most commonly adopt six-coordinated octahedral geometry [22, 23], five-coordinated square-pyramidal geometry and seven-coordinated pentagonal bipyramidal geometry [24, 25], and four-coordinated mode is adopted when the volume of ligand is very large [26]. At the same time, researches have showed that the N atom of imidazolyl have strong coordination ability and can coordinated with multiple metal salts [27]. Different anions have a big effect on the coordination mode of the central ions and the packing architecture of the com-

Table 2. Selected bond distances (Å) and angles (deg) for **I**–**III***

Bond	*d*, Å	Bond	*d*, Å
I			
Cd(1)–O(2)	2.323(2)	Cd(1)–N(4)	2.298(2)
Cd(1)–O(3)	2.337(2)		
II			
Cd(1)–N(1)	2.241(3)	Cd(1)–Br(1)	2.5705(9)
III			
Cd(1)–N(4)	2.239(4)	Cd(1)–I(1)	2.7472(9)
Angle	ω, deg	Angle	ω, deg
I			
N(4)Cd(1)O(2)	87.56(8)	N(4)$^{\#1}$Cd(1)O(2)$^{\#1}$	87.56(8)
O(2)Cd(1)O(3)	88.65(9)	N(4)Cd(1)O(3)	88.14(8)
O(2)Cd(1)O(3)$^{\#1}$	91.35(9)	N(4)Cd(1)O(3)$^{\#1}$	91.86(8)
N(4)$^{\#1}$Cd(1)O(2)	92.44(8)		
II			
N(1)Cd(1)N(1)$^{\#1}$	102.76(14)	N(1)Cd(1)Br(1)$^{\#1}$	123.26(8)
N(1)Cd(1)Br(1)	98.19(8)	Br(1)Cd(1)Br(1)$^{\#1}$	112.79(4)
III			
N(4)Cd(1)N(4)$^{\#1}$	105.0(2)	N(4)Cd(1)I(1)	122.26(10)
N(4)$^{\#1}$Cd(1)I(1)	97.79(11)	I(1)$^{\#1}$Cd(1)I(1)	113.30(5)

* Symmetry transformations used to generate equivalent atoms: $^{\#1}$ $-x + 3, -y + 1, -z$ (I); $^{\#1}$ $-x + 1, y, -z + 3/2$ (II); $^{\#1}$ $-x + 2, y, -z + 5/2$ (III).

plexes, a mount of diversiform supermolecules containing imidazolyl with different anions (CH_3COO^-, SCN^-, SO_4^{2-}, Br^-, etc.) have been reported and analyzed [28, 29].

In complex **I**, the cadmium atom resides in an ideal octahedral environment with two oxygen atoms from two water molecules at the apical positions, and two oxygen atoms from different acetate anions and two nitrogen atoms from two different ligands at the equatorial positions. According to previous reports and current results, the coordinated water molecules play a key role in the coordination mode of Cd(II) [30]. Without the coordinated water molecules, acetate anions maybe adopt the bidentate coordination mode to form four-membered chelate ringlike structure. Water molecule should be considered as an important factor in the design of metal-organic structures due to most metal salts containing crystal water molecules.

The anion acts as a key role in determining the structures of the resultant complexes. Halogen ions have been widely used as anions for the construction of the metal coordination complexes because they can adjust the topologies of complexes through different coordinate bonds or non-covalent interactions [31, 32]. In the paper, when we used halogen ions (Br^-, I^-) instead of CH_3COO^-, the coordination mode of Cd atom and the structure of aggregates all take place a significant change. First of all, the coordination environment of the central Cd atom change from six-coordinated octahedral geometry in complex **I** into four-coordinated slight distorted tetrahedral geometry of complex **II** and **III**, which may be due to the strong coordination ability and relatively large ionic radius of halogen ions. Secondly, the higher-dimensional structures are different, complexes **II** and **III** display the similar framework structures, the two ligands coordinated with the central metal ion construct a V-type structure and extend in [010] to form the one-dimensional chains. The chains linked together through C–H···N interactions to generate a 2D framework. However in complex **I**, two cyano groups of a line-type structure

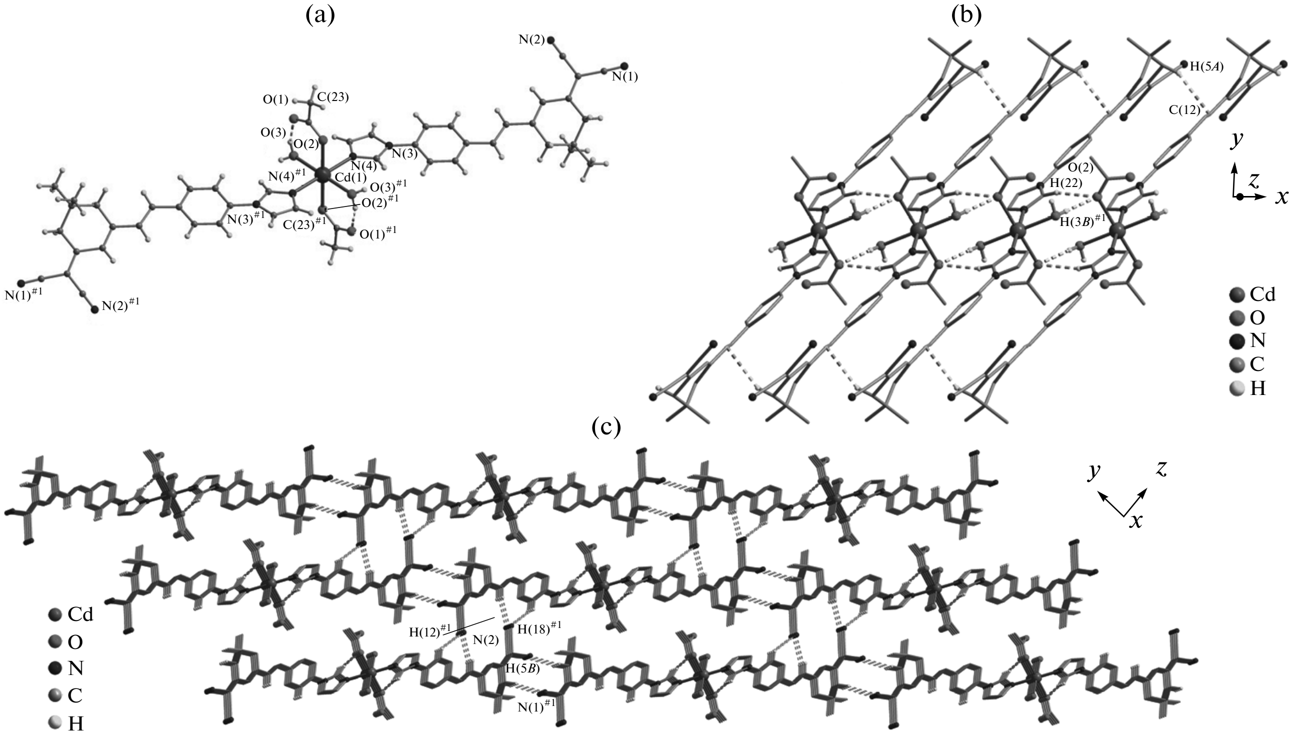

Fig. 1. Molecular structure of complex **I** (a); the one-dimensional structure of complex **I** (b). The three-dimensional structure of complex **I** viewed along *x* axis (c). Dotted lines represent the weak interactions. Symmetry code: $^{\#1}$ $-x + 3, -y + 1, -z$.

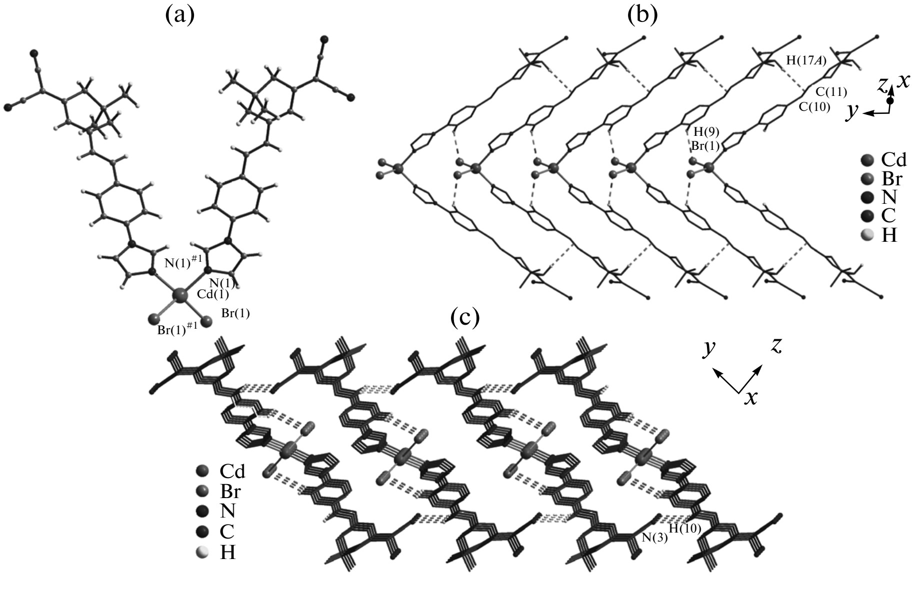

Fig. 2. Molecular structure of complex **II** (a); the one-dimensional structure of complex **II** (b); the two-dimensional structure of complex **II** viewed along *y* axis (c). Dotted lines represent the weak interactions. Symmetry code: $^{\#1}$ $-x + 1, y, -z + 3/2$.

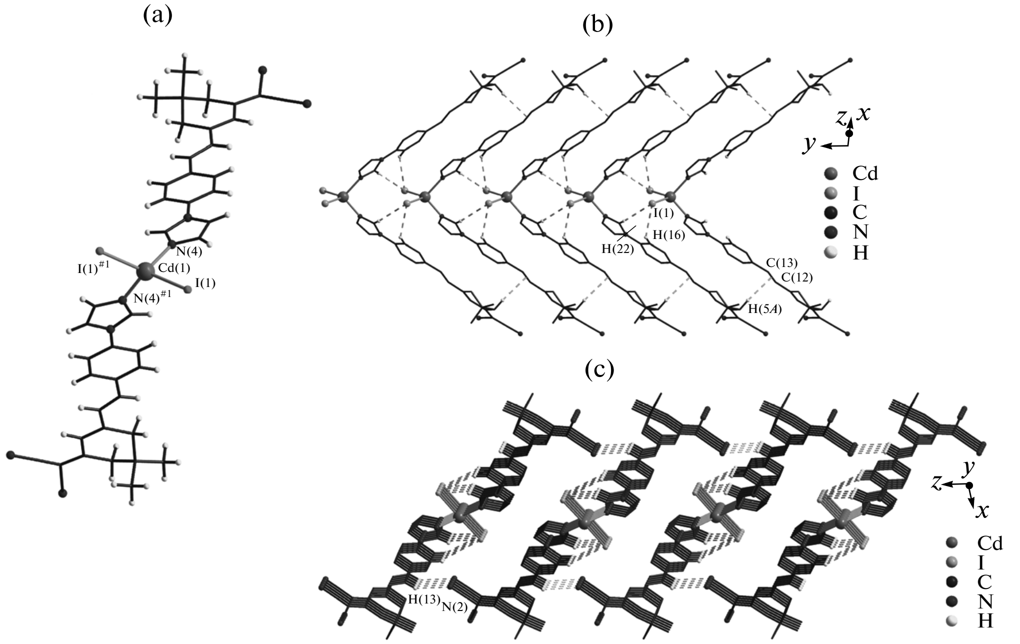

Fig. 3. Molecular structure of complex **III** (a); the one-dimensional structure of complex **III** (b); the two-dimensional structure of complex **III** viewed along y axis (c). Dotted lines represent the weak interactions. Symmetry code: $^{\#1}$ $-x + 2, y, -z + 5/2$.

make use of hydrogen bonding interaction to form 2D layers and 3D structure, respectively.

Coordination complexes with d^{10} metal atoms show fluorescence properties and are promising candidates for photoactive materials with potential applications. For potential applications as luminescent materials, the luminescent properties of the three complexes have been investigated in the solid state at room temperature.

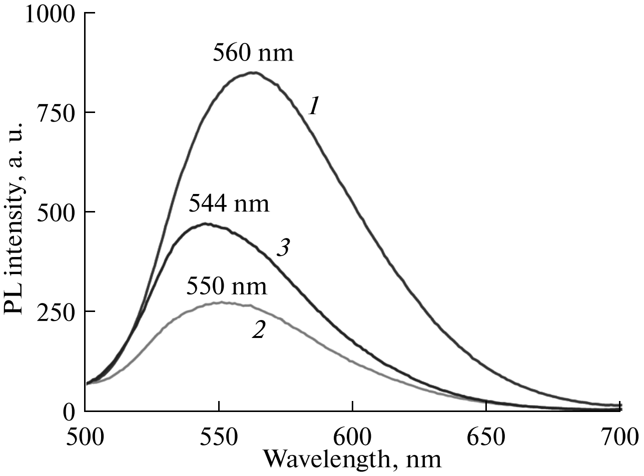

Fig. 4. Solid-state emission spectra of complexes **I** (*1*), **II** (*2*), and **III** (*3*) at room temperature, the pass width are 5 nm.

The complexes are excited at the excitation wavelength of 468 nm. Figure 4 presents the emission spectra, complex **I** exhibits the maximum emission peak at 560 nm. The maximum emission peaks of **II** and **III** are blue shifted to 550 and 544 nm, respectively. The fluorescence decay profiles of the three complexes were measured at their optical excitation wavelengths in the solid state at room temperature. The fluorescence lifetimes of **I**, **II**, and **III** are all less than 0.1 ns.

To get better understanding the relationship between the optical properties and electronic structure, we performed theoretical calculations on their energy levels by density functional theory (DFT) method at B3LYP/6-31G(d) based on the molecular conformation in crystal structure. Their highest occupied molecular orbital (**HOMO**) and lowest unoccupied molecular orbital (**LUMO**) plots of complexes **I–III** are shown in Fig. 5. Their electron distribution of HOMO and LUMO are similar. The most of electron clouds of the HOMO are distributed on the anions (Br^-, I^-, CH_3COO^-), while the major electron clouds of the LUMO are transferred and distributed on the ligand. The results suggest that the emission bands are mainly originally from the intramolecular charge transfer. Therefore the electron-withdrawing ability of CH_3COO^- is weaker than that of Br^- and I^-, the maximum emission peak of complex **I** is the longest. In the same way, the maximum emission peaks of **II** exhibit red shift of 6 nm compared with that of **III**.

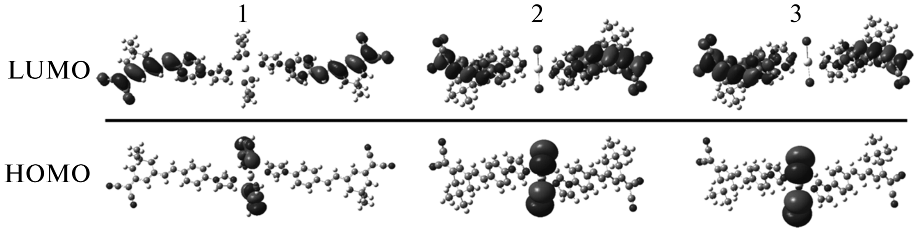

Fig. 5. Electron density distributions of the frontier molecular orbitals of complexes **I** (1), **II** (2), and **III** (3).

ACKNOWLEDGMENTS

This work was supported by the Program for New Century Excellent Talents in University (China), the Doctoral Program Foundation of the Ministry of Education of China (20113401110004), the National Natural Science Foundation of China (21271003 and 21271004), the Natural Science Foundation of Education Committee of Anhui Province (KJ2012A024), the 211 Project of Anhui University, the Ministry of Education Funded Projects Focus on Returned Overseas Scholar and Dr Start-up funds of Anhui University (33190077, 33190224).

REFERENCES

1. Xie, Y.P., Yang, J., Ma, J.F., et al., *Cryst. Growth Des.*, 2009, vol. 9, no. 9, p. 3881.
2. Guha, S., Drew, M.G., and Banerjee, A., *Cryst. Growth Des.*, 2010, vol. 10, no. 11, p. 4716.
3. Corma, A., Garcia, H., and Llabrés i Xamena, F., *Chem. Rev.*, 2010, vol. 110, no. 8, p. 4606.
4. Liu, Q.K., Ma, J.P., and Dong, Y.B., *Chem. Commun.*, 2011, vol. 47, p. 12343.
5. Jin, F., Zhang, Y., Wang, H.Z., et al., *Cryst. Growth Des.*, 2013, vol. 13, p. 1978.
6. Yan, D., Patel, B., Delory, A., et al., *Cryst. Growth Des.*, 2013, vol. 13, p. 333.
7. Ebenezer, S., Muthiah, P.T., and Butcher, R.J., *Cryst. Growth Des.*, 2011, vol. 11, p. 3579.
8. Liu, Y., Zhao, Y.L., Zhang, H.Y., et al., *Macromolecules*, 2004, vol. 37, no. 17, p. 6362.
9. Richards, V.J., Argent, S.P., Kewley, A., et al., *Dalton Trans.*, 2012, vol. 41, p. 4020.
10. Fang, S.M., Zhang, Q., Hu, M., et al., *Inorg. Chem.*, 2010, vol. 49, no. 20, p. 9617.
11. Plessis, M. du and Barbour, L.J., *Dalton Trans.*, 2012, vol. 41, p. 3895.
12. Tedesco, C., Erra, L., Immediata, I., et al., *Cryst. Growth Des.*, 2010, vol. 10, no. 4, p. 1527.
13. Luo, L., Chen, K., Liu, Q., et al., *Cryst. Growth Des.*, 2013, vol. 13, p. 2312.
14. Li, G.B., Liu, J.M., Cai, Y.P., et al., *Cryst. Growth Des.*, 2011, vol. 11, p. 2763.
15. Morrison, C.N., Powell, A.K., and Kostakis, G.E., *Cryst. Growth Des.*, 2011, vol. 11, p. 3653.
16. Hou, S., Liu, Q.K., Ma J.P., et al., *Inorg. Chem.*, 2013, vol. 52, p. 3225.
17. Shin, J.W., Bae, J.M., Kim, C., et al., *Inorg. Chem.*, 2013, vol. 52, p. 2265.
18. Jin, F., Wang, H.Z., Zhang, Y., et al., *CrystEngComm*, 2013, vol. 15, p. 3687.
19. Zaman, M.B., Udachin, K.A., and Ripmeester, J.A., *Cryst. Growth Des.*, 2004, vol. 4, p. 585.
20. Zheng, Z., Yu, Z.P., Yang, M.D., et al., *J. Org. Chem.*, 2013, vol. 78, p. 3222.
21. Sheldrick, G.M., *SADABS, A Program for Exploiting the Redundancy of Area-Detector X-ray Data,* Göttingen (Germany): Univ. of Göttingen, 1999.
22. Wei, G.H., Yang, J., Mang, J.F., et al., *Dalton Trans.*, 2008, vol. 29, p. 3080.
23. Zhao, W., Fan J., Okamura, T.A., et al., *New J. Chem.*, 2004, vol. 28, p. 1142.
24. Wang, L., Yan, Z.H., Xiao, Z.Y., et al., *CrystEngComm*, 2013, vol. 15, p. 5552.
25. Kuai, H.W., Fan, J., Liu, Q., et al., *CrystEngComm*, 2012, vol. 14, p. 3708.
26. Alvarez, H.M., Tran, T.B., Richter, M.A., et al., *Inorg. Chem.*, 2003, vol. 42, no. 6, p. 2149.
27. Li, C.Y., Liu, C.S., Li, J.R., et al., *Cryst. Growth Des.*, 2007, vol. 7, no. 2, p. 286.
28. Bai, H.Y., Ma, J.F., Yang J., et al., *Cryst. Growth Des.*, 2010, vol. 10, no. 2, p. 995.
29. Kimblin, C. and Parkin, G., *Inorg. Chem.*, 1996, vol. 35, no. 24, p. 6912.
30. Zhang, S., Lan, J., Mao, Z., et al., *Cryst. Growth Des.*, 2008, vol. 8, no. 9, p. 3134.
31. Du, M., Chen, S.T., and Bu, X.H., *Cryst. Growth Des.*, 2002, vol. 2, no. 6, p. 625.
32. Ma, Q., Zhu, M., Yuan, C., et al., *Cryst. Growth Des.*, 2010, vol. 10, no. 4, p. 1706.